

## Article

# Effect of Potential and Chlorides on Photoelectrochemical Removal of Diethyl Phthalate from Water

Laura Mais , Simonetta Palmas , Michele Mascia  and Annalisa Vacca \*

Dipartimento di Ingegneria Meccanica, Chimica e dei Materiali, Università degli Studi di Cagliari, Via Marengo 2, 09123 Cagliari, Italy; laura.mais@unica.it (L.M.); simonetta.palmas@dimcm.unica.it (S.P.); michele.mascia@unica.it (M.M.)

\* Correspondence: annalisa.vacca@dimcm.unica.it

**Abstract:** Removal of persistent pollutants from water by photoelectrocatalysis has emerged as a promising powerful process. Applied potential plays a key role in the photocatalytic activity of the semi-conductor as well as the possible presence of chloride ions in the solution. This work aims to investigate these effects on the photoelectrocatalytic oxidation of diethyl phthalate (DEP) by using TiO<sub>2</sub> nanotubular anodes under solar light irradiation. PEC tests were performed at constant potentials under different concentration of NaCl. The process is able to remove DEP following a pseudo-first order kinetics: values of  $k_{app}$  of  $1.25 \times 10^{-3} \text{ min}^{-1}$  and  $1.56 \times 10^{-4} \text{ min}^{-1}$  have been obtained at applied potentials of 1.8 and 0.2 V, respectively. Results showed that, depending on the applied potential, the presence of chloride ions in the solution affects the degradation rate resulting in a negative effect: the presence of 500 mM of Cl<sup>-</sup> reduces the value of  $k_{app}$  by 50 and 80% at 0.2 and 1.8 V respectively.

**Keywords:** diethyl phthalate; photoelectrochemical degradation; persistent organic pollutants; chloride ions; TiO<sub>2</sub> nanotubes



**Citation:** Mais, L.; Palmas, S.; Mascia, M.; Vacca, A. Effect of Potential and Chlorides on Photoelectrochemical Removal of Diethyl Phthalate from Water. *Catalysts* **2021**, *11*, 882. <https://doi.org/10.3390/catal11080882>

Academic Editor: Bruno Fabre

Received: 17 June 2021

Accepted: 19 July 2021

Published: 22 July 2021

**Publisher's Note:** MDPI stays neutral with regard to jurisdictional claims in published maps and institutional affiliations.



**Copyright:** © 2021 by the authors. Licensee MDPI, Basel, Switzerland. This article is an open access article distributed under the terms and conditions of the Creative Commons Attribution (CC BY) license (<https://creativecommons.org/licenses/by/4.0/>).

## 1. Introduction

The application of photoelectrochemical process for polluted waters and wastewaters has been gaining more and more attention thanks to the possibility to obtain electrical energy from renewable energy sources, rather than from fossil fuels [1]. The technique exploits the synergy between photochemistry and electrochemistry: from one side, the photochemical process increases its efficiency as the bias potential lowers recombination of the photogenerated charges, from the other side the photo-potential generated on the semiconductor depolarizes the cell improving the yield of the electrochemical process [2].

Considering the application to real matrices, the effect of the composition of the water to be treated plays a crucial role, with particular regard to the presence of chlorides, which are ubiquitous ions in water and wastewater. Several studies on the photochemical process using TiO<sub>2</sub> highlighted a negative effect of the presence of chloride: the inhibiting effect has been ascribed both to the competitive adsorption between the pollutant molecules and Cl<sup>-</sup> towards the surface-active sites of TiO<sub>2</sub>, or to the scavenging function of chloride ions towards holes and hydroxyl radicals [3,4]. Piscopo et al. [5] showed different effects on the degradation rate of two pollutants depending on the chloride concentration, the nature of the organics and the pH: in the case of poorly adsorbed molecules, if the pH favored the adsorption of Cl<sup>-</sup>, even low concentration of chloride strongly affected the degradation.

Several papers evidenced the key role of pH in the photocatalytic degradation using TiO<sub>2</sub>: point of zero charge (pH<sub>pzc</sub>) plays a crucial role in determining the surface charge of photocatalyst and, in turn, its interaction with charged molecules or ions. When the pH is higher than the pH<sub>pzc</sub>, the polarity of TiO<sub>2</sub> surface is negative and the electrostatic repulsion toward anionic compounds dominates [6–8]. Moreover, since hydroxyl radicals can be formed by the reaction between hydroxide ions and positive holes, the hydroxyl radicals are

considered as the predominant species at neutral or high pH, while at low pH the holes are considered the major oxidizing species [9]. Regarding the scavenging effect, chloride can react with HO• radicals and holes, allowing the formation of less reactive chloride radical (Cl•) and dichloride radicals (Cl<sub>2</sub>•<sup>-</sup>) [10–12]: the oxidized chloride may also recombine with photogenerated electrons quenching the photogenerated charge carriers [13].

Different considerations may be made when photoelectrocatalysis is considered: in this case, heterogenous photocatalysis can be improved by the application of a bias potential to obtain a more effective separation of photogenerated charges, thereby increasing the lifetime of electron–hole pairs. In the photoelectrocatalytic process, the increases of the applied potential can accelerate the photogenerated electrons toward the external circuit, generating the bending of the conduction and valence bands, with the consequent formation of a space charge layer. Thus, the recombination of the e<sup>-</sup>/h<sup>+</sup> pairs may be decreased or totally prevented, improving the photocatalytic performance [14,15]. Moreover, increase in the potential can empty the defects where the photogenerated charges are trapped, enhancing the photoactivity [16].

The presence of chloride in a photoelectrochemical process exerts a different effect with respect to the photochemical one: in fact, unlike the inhibitory effects found in photocatalysis, in photoelectrochemical removal of pollutants, enhancing effect in the degradation process has been often highlighted. Zanoni et al. [17] reported the highest discoloration rate and TOC removal for solution containing Remazol Brilliant Orange 3R at pH 6.0 in presence of 0.5 M of NaCl applying +1.0 V (SCE) to the TiO<sub>2</sub> photoanode. Also, in the case of other dyes or organics, the presence of Cl<sup>-</sup> has been found beneficial to accelerate the degradation rate [18,19]. The improvement in the degradation has been explained by the synergistic action of the strong oxidizing species HO•, chlorine-based radicals Cl• and Cl<sub>2</sub>•<sup>-</sup>, and active chlorine species like HClO and Cl<sub>2</sub> that can give a bulk contribution [20,21]. Moreover, at the anode the adsorption of negative charged ions, such as chloride, can be enhanced both by the polarization and the promotion of reactions that can generate local acidic pH variation near the anodic surface.

In this framework, our work is devoted to study the photoelectrochemical degradation of a persistent organic pollutant at two levels of applied potentials and in the presence of different concentrations of chloride under simulated solar light conditions, using TiO<sub>2</sub> nanotubular electrodes. The pollutant selected for the study is the diethylphthalate (DEP). Phthalate esters (PAEs) are a group of widely used plasticizers that can lead to endocrine system disorders, affecting reproductive function, and inducing some tumors [22–24]. Due to their wide utilization and the difficulty to completely remove them with conventional treatment processes, PAEs are ubiquitous persistent organic pollutants in the environment, being the short chain phthalate as DEP, the most detected in surface marine waters, freshwaters, and sediments [25–27]. To the best of our knowledge, only few papers reported on the photoelectrochemical degradation of the diethyl phthalate [28,29]. Moreover, the influence of the presence of chloride during their treatment and the effect of the applied potential are not yet presented by the literature.

## 2. Materials and Methods

### 2.1. Preparation of TiO<sub>2</sub> Nanotubes

TiO<sub>2</sub> nanotube electrode (TiO<sub>2</sub>-NT) used for the photoelectrochemical degradation of DEP was prepared by electrochemical anodization as reported in our previous work [30]. Briefly, Ti foils (0.25 mm thickness, 99.7% metal basis, Aldrich, St. Louis, MO, USA) were cut in circular disks of 5 cm diameter. After ultrasonic treatments in acetone, isopropanol and methanol (10 min each), Ti was rinsed with deionized water, and dried with a nitrogen stream. The anodization was performed in a two-electrode cylindrical cell made by Teflon (inner dimension: diameter = 4.4 cm and height = 5 cm). The working electrode was located at the bottom of the cell where the electrical contact was an aluminum disc. The exposed geometrical area of the Ti electrodes was 15 cm<sup>2</sup>. A platinum titanium grid placed in front of the anode at 1 cm distance constituted the counter electrode.

The anodization was performed in (10%) deionized water/(90%) glycerol solution with 0.14 M of  $\text{NH}_4\text{F}$  at room temperature. A potential ramp was imposed from open circuit voltage (OCV) to 20 V with a scan rate of  $100 \text{ mVs}^{-1}$ ; then the applied potential was maintained at this fixed value for 4 h.  $\text{TiO}_2$ -NT was annealed in air atmosphere at  $400^\circ\text{C}$  for 1 h to transform the amorphous structure into crystalline one. The phase transformation depends on both the structure morphology and annealing temperature: it has been shown that the anatase-to-rutile transformation starts near  $430^\circ\text{C}$  for the 500 nm long nanotubes [31], while the same transformation has been reported to occur at  $550^\circ\text{C}$  for nanotubes up to 200 nm [32]. In our case, after 1 h at  $400^\circ\text{C}$ , a unique anatase phase was present [33]. The morphological characterization of  $\text{TiO}_2$ -NT was presented in [30]: the average diameter of tubes ranged between 40–50 nm, while the tube length of around 700 nm was measured.

## 2.2. Photoelectrochemical Tests

Photoelectrochemical tests were performed in a three-electrode beaker cell using  $\text{TiO}_2$  nanotubes as photoanode, a platinized titanium grid as cathode, and a saturated calomel electrode (SCE) as reference. The cell was filled with 100 mL of solution and connected with a potentiostat-galvanostat (Metrohm Autolab 302N, Metrohm, Herisau, Switzerland) controlled by Nova software. The photoanode was irradiated by UV-vis light using a 300 W xenon lamp equipped with air mass (AM) 0 and 1.5 D filters to simulate the solar irradiation.

Photocurrent measurements were carried out by linear sweep voltammetric (LSV) runs, starting from the OCV to 2.5 V at a scan rate of  $10 \text{ mVs}^{-1}$ , with hand-chopped light. The photocurrent-time measurements were recorded applying a constant potential in the dark for 10 min; afterward, the electrode was exposed to light for 200 s, followed by dark condition.

Photoelectrochemical oxidation of diethyl phthalate was performed under potentiostatic conditions at 0.2 and 1.8 V vs. SCE. The initial concentration of the organic compound was  $40 \text{ mg dm}^{-3}$  and 0.1 M  $\text{NaClO}_4$  was used as supporting electrolyte. Moreover, different amount of NaCl (1, 100, 500 mM) were added to the solution, to investigate on the effect of chloride concentration during the photoelectrochemical oxidation of DEP. The pH of the solution was neutral. During degradation experiments, samples of electrolyte were withdrawn for qualitative and quantitative analyses of the model organic compound.

## 2.3. Analytical Methods

Analyses of the model organic compound were carried out by HPLC (Waters), equipped with a column Varian C18 and a dual band UV detector set to 283 and 229 nm. The mobile phase was Acetonitrile and aqueous solution 0.1%  $\text{H}_3\text{PO}_4$  = 40:60 with a flow rate of  $1 \text{ mL min}^{-1}$ .

The oxidant concentration, expressed as  $\mu\text{M}$  of active chlorine, was measured using the N,N-diethyl-p-phenylenediamine (DPD) colorimetric method. DPD oxidizes to form a red-violet product, the concentration of which is determined measuring the absorbance at 515 nm.

The trend of mineralization was monitored by measuring the total organic carbon (TOC) by a Shimadzu TOC 500L instrument.

For each sample a repeatability within  $\pm 5\%$  has been evaluated.

## 3. Results and Discussion

Figure 1 shows the trend of polarization curve performed at the  $\text{TiO}_2$ -NT electrode during LSV in aqueous solution of DEP under irradiation and in the dark.

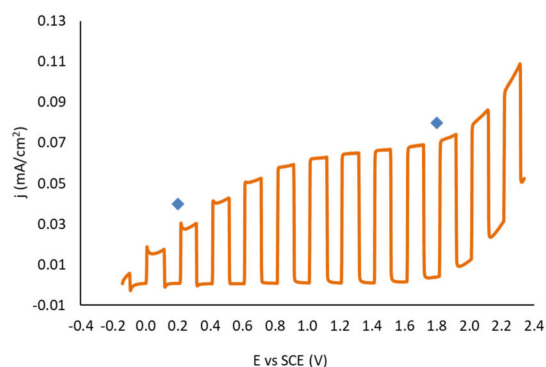


**Figure 1.** LSV of TiO<sub>2</sub>-NT performed at 10 mV s<sup>-1</sup> of scan rate, under dark and irradiation condition. Blue symbols indicate the potentials selected for the degradation runs.

A typical trend is observed, with an onset potential of  $-0.25$  V, followed by an ohmic behavior of the system, in which the positive influence of the potential is strictly connected to the increase in the space charge depletion region of the semiconductor; in the central range of potential (0.7–1.8 V) the saturation of the current is reached, in which increase of the potential is no more effective in terms of a corresponding increasing of the current. In the final range, at potentials higher than the value of band gap of the semiconductor, the barrier breakdown effect could be responsible for the sharp rising in the photocurrent along with the dark current contribution [30].

The degradation tests have been performed selecting two applied potentials: the first one in the ohmic region and the second one in the saturation region. The two blue diamonds in Figure 1 indicate the values of potential selected.

Figure 2a shows the trend with time of the DEP concentration, normalized with respect to the initial concentration, during electrolysis at the two different potentials. For comparison, the trend with time of the DEP concentration at the open circuit potential in the dark was also reported in the same figure: no significant adsorption of DEP on the electrode surface was detected that can be explained considering the neutral pH of the solution, the iso-electrical point of TiO<sub>2</sub> located around pH = 6, and the non-ionic nature of the molecule of DEP. When the runs were performed in potentiostatic conditions and under illumination, the concentration of DEP decreased, being the highest reaction rate achieved at 1.8 V.

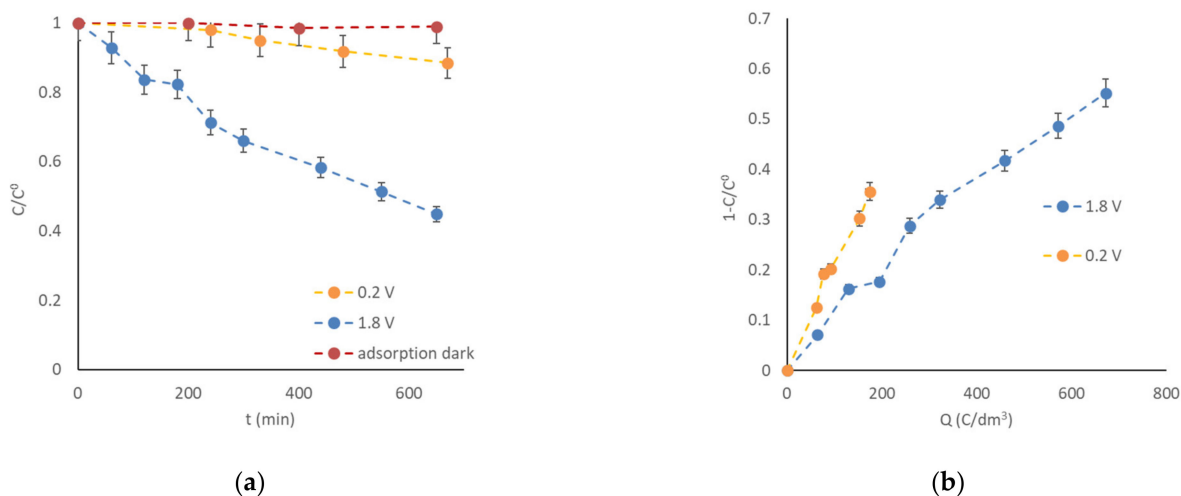


**Figure 2.** (a) Trends with time of the concentration of DEP, normalized to the initial concentration  $C^0$ , during runs performed with solutions containing 40 mg dm<sup>-3</sup> DEP in 0.1 M NaClO<sub>4</sub> as supporting electrolyte at different applied potentials. (b) Fraction of reactant removed as a function of the specific charge supplied during the related runs.

However, since the mean current intensity measured during the potentiostatic runs was 0.1 mA at 0.2 V and 1.2 mA at 1.8 V, it could be useful to compare the trend of fraction of the removed reactant as a function of the specific supplied charge (Figure 2b): in this case, the highest yield of the removal process is measured at the lowest potential, indicating that most of the charge passed at 1.8 V has been used for the side reaction of water oxidation.

An analogous behavior was observed in our previous work, where the photo-electrocatalytic degradation of 2,4-dichlorophenoxyacetic acid was investigated: higher efficiency and slower kinetics of degradation were detected in the ohmic region of the polarization curve with respect to those in the saturation region [30].

Degradation curves of DEP at various chloride concentration at the two applied potentials are shown in Figure 3a,b as semilogarithmic plots. A linear trend of  $\ln(C/C^0)$  vs. time is observed under all the experimental conditions, indicating that a pseudo-first order kinetics could be used to interpret the data, as follows:

$$dC/dt = -k_{app} C \quad (1)$$

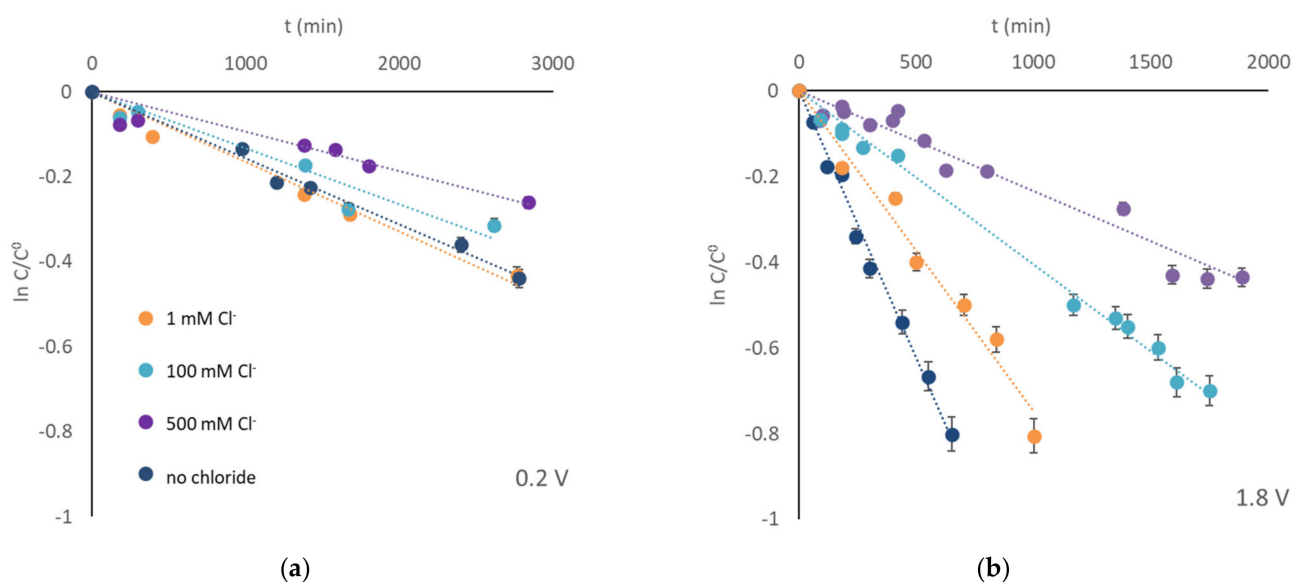


**Figure 3.** Trends with time of  $\ln C/C^0$  during photoelectrochemical degradations using solutions containing 40 mg  $dm^{-3}$  DEP, 0.1 M  $NaClO_4$ , and different chloride concentration. (a) Applied potential: 0.2 V; (b) applied potential: 1.8 V.

The values of the apparent kinetic constant  $k_{app}$ , evaluated from the slope of each straight line at the relevant operative conditions are reported in Figure 4, as a function of the chloride concentration. As already observed in absence of chloride, the fastest kinetics of the reactant removal are obtained at 1.8 V for each level of chloride concentration. Moreover, at 0.2 V, the increase of chloride concentration scarcely affects the reaction rate, except for 500 mM of  $Cl^-$ , which halves the  $k_{app}$ . At 1.8 V, the effect of chloride is more evident: at 1 mM of  $Cl^-$  the  $k_{app}$  is reduced by 40% while at 500 mM of  $Cl^-$  by 80%, in respect to the  $k_{app}$  evaluated without chloride.

Figure 5 shows the trend of the ratio between  $k_{app}$  evaluated at 1.8 V and that at 0.2 V measured at different chloride concentrations. In absence of chloride, an increment of one order of magnitude is obtained, while in presence of the highest concentration of chloride  $k_{app}$  increases of two-fold when the potential values change from 0.2 to 1.8 V. This behavior indicates that the higher the potential, the higher is the negative effect of the concentration of chloride.

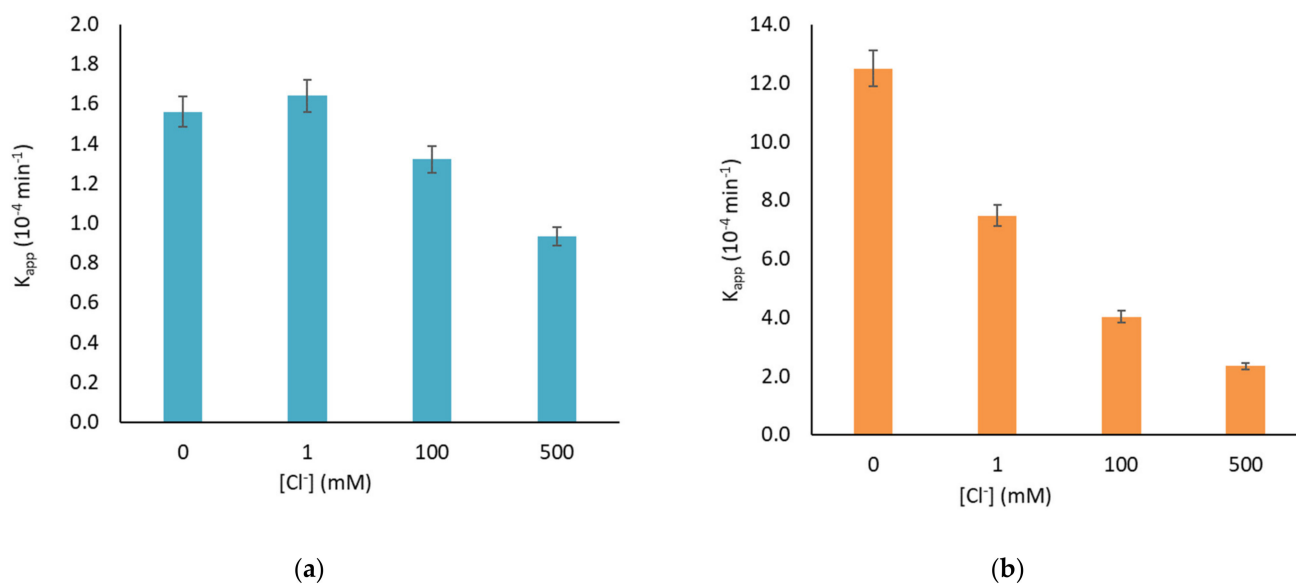


**Figure 4.** Pseudo-first order kinetic constants of the reactant removal process performed in solutions of  $40 \text{ mg dm}^{-3}$  of DEP,  $0.1 \text{ M NaClO}_4$ , and different chloride concentration. (a) Applied potential:  $0.2 \text{ V}$ ; (b) applied potential:  $1.8 \text{ V}$ .

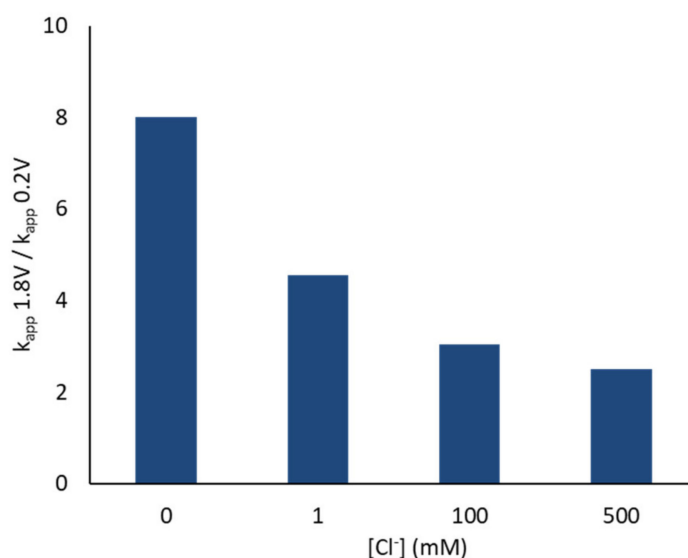


**Figure 5.** Ratio between the apparent kinetic constant evaluated at  $1.8$  and  $0.2 \text{ V}$  for different chloride concentrations.

The inhibiting effect observed in presence of  $\text{Cl}^-$  agrees with observations reported for photocatalytic processes at  $\text{TiO}_2$ -based materials. Several mechanisms have been proposed to explain the inhibiting effect on the photocatalytic degradation [13]:

- (1) scavenging of holes or  $\text{HO}\bullet$  radicals by chloride ions [34–36].
- (2) blocking of active surface sites by chloride ions [3,20,37].
- (3) chloride acting as surface-charge-recombination center for photogenerated charge carriers [38].

Moreover, due to the complexity of the processes, a combination of mechanisms is often claimed to explain the inhibiting effect [5,13,39–41].

In the case of a photo-electrochemical process, also the effect of the applied potential should be considered, as well as the pH modification due to the side reactions that occur to a greater or lesser extent depending on the applied potential.

In order to verify the effect of the concentration of chloride and the applied potential on the behavior of the semiconductor, photocurrent transients have been recorded applying different potential and varying the chloride concentration during chopped light chronoamperometries.

Figure 6 shows the results obtained without chloride. For TiO<sub>2</sub> nanotubes, the thickness of the wall can be determinant for the extension of the space charge depletion layer; this in turn, can be relevant for the recombination phenomena, which are strictly connected to the applied potential. As can be seen, at the lowest potential, a typical spike of the anodic current is observed, followed by an exponential decrease of the photocurrent with time until a stationary value is reached. The positive spike is no more visible at the highest potential. According to the literature [42], the positive current transient when the light is turned on represents the accumulation of holes at the electrode/electrolyte interface without injection to the electrolyte. Since any fast faradic reaction is occurring, the charge recombination is responsible for the subsequent decrease of the measured current.

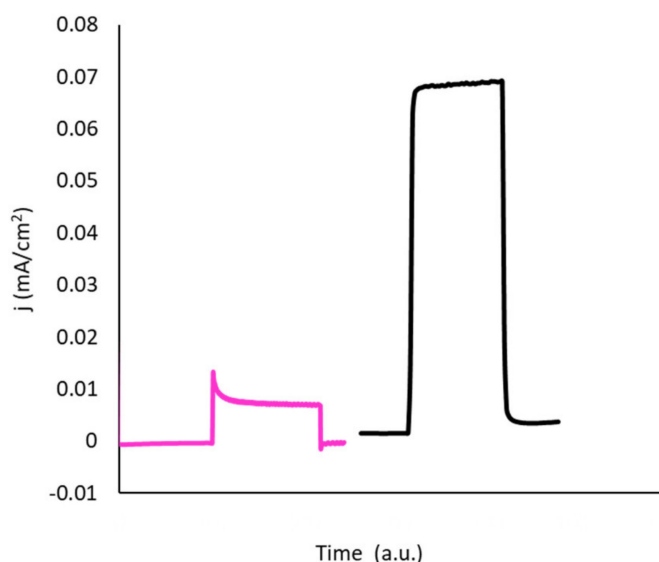


**Figure 6.** Potentiostatic tests performed with solution containing 0.1 M NaClO<sub>4</sub> at 0.2 (pink) and 1.8 V (black).

At low potentials, when we operate in the ohmic region of the polarization curve, where the charge depletion layer thickness is not fully developed inside the nanotubes wall, the photogenerated holes may rapidly recombine in the regions of the material that do not experience beneficial space charge effects, i.e., that are non-depleted of the majority carriers (electrons). When the experiment is performed at the highest potential (in the saturation region of the polarization curve) the depletion layer extends in the whole wall of nanotubes and the recombination is suppressed.

Photocurrent transients in presence of chloride are reported in Figure 7.

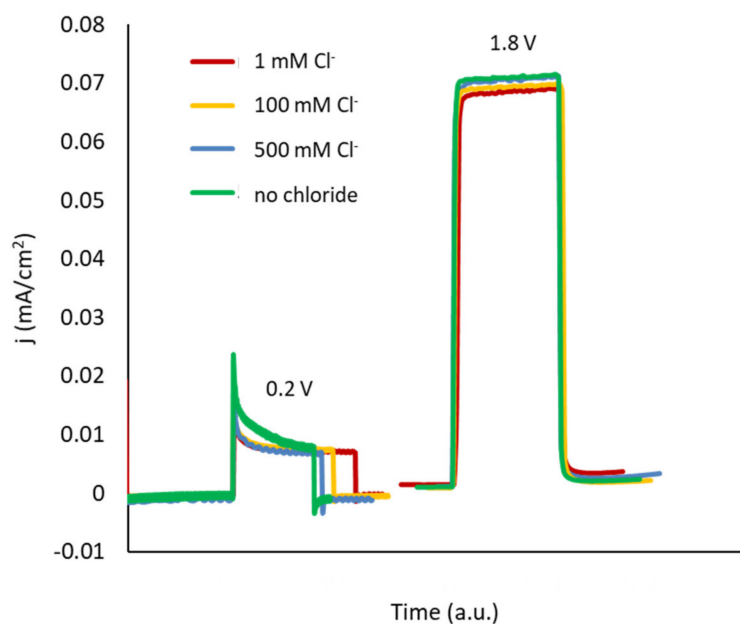


**Figure 7.** Potentiostatic tests performed with solution containing 0.1 M NaClO<sub>4</sub> and different concentration of chloride ions at 0.2 and 1.8 V.

At low applied potential, the rate of the photocurrent decreasing (i.e., the rate of the charge recombination process) is scarcely influenced by the presence of chloride, when they are present at low concentration levels: overlapped curves are obtained related to the runs performed at 0, 1, and 100 mM of Cl<sup>−</sup> ions. Only at 500 mM of Cl<sup>−</sup>, slower decay of the photocurrent can be observed, indicating an inhibition of the recombination processes. Moreover, when the light was turned off, negative current transients were observed for high chloride concentration. Negative spikes were often detected during photocurrent transient of semiconductors and can be related to slower electron/hole pairs recombination due to the presence of holes trapped in the surface [43].

These transients in photocurrent can be explained as follows: at lower chloride concentration, the charge recombination prevails since chloride is poorly adsorbed onto the semiconductor electrode, so it is not able to react with the photogenerated holes faster than the electrons. However, at the highest concentration of chloride, it is likely that the adsorption effect would predominate, so that chloride can act as hole scavenger, according to the following adsorption phenomena:



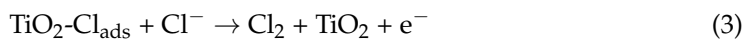
This process promotes the separation of electron-hole pair limiting the charge recombination as suggested by other authors [20,44,45].

At the highest potential, the recombination is suppressed, and positive transient and negative spikes disappear also in presence of high chloride ions. Moreover, very small increment in the steady state photocurrent was observed, increasing the concentration of chloride. So, at 0.2 V, the highest variation in the value of  $k_{\text{app}}$  obtained at 500 mM of chloride, can be connected to the blocking effect of adsorbed Cl<sup>−</sup> and the competitive adsorption, with respect to water molecules, which reduces the formation of HO• radicals.

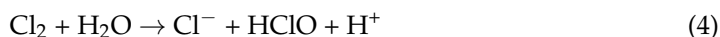
Similar considerations should be done also to explain the result at 1.8 V, but, as we noticed, the inhibiting effect at this potential is evident also at low concentration of chloride. This can be explained by considering two aspects connected to the applied potential: the electrode works in a region of potential where the oxygen evolution reaction occurs to a large extent, so that a local acidic pH near the surface can generate a positive charge (pH < isoelectric point). Moreover, the application of high anodic potentials can generate a build-up of a positive surface charge. In this condition, the competitive adsorption or

blocking of active surface sites by chloride anions will be favored due to the electrostatic attraction of  $\text{Cl}^-$ , also at low concentration of chloride.

The adsorbed chloride can react to form chlorine by the following reaction [17,44]:



Dissolved chlorine reacts with water to give hypochlorous acid and hypochlorite ions (Equations (3) and (4)), being the distribution of the three forms of active chlorine dependent on pH:



Chlorine-based oxidants (active chlorine) have been detected during the photoelectrochemical degradation of DEP in different operating conditions.

At 0.2 V after  $130 \text{ C dm}^{-3}$  of supplied charge, 2.0 and 4.2  $\mu\text{M}$  of active chlorine concentrations were detected at 100 and 500 mM of  $\text{Cl}^-$ , respectively. These small amounts agree with the poor adsorption of chloride at this value of applied potential. At 1.8 V, higher concentration of active chlorine was detected. As an example, the trend with time of the concentration of active chlorine obtained during DEP degradation in presence of 100 mM of  $\text{Cl}^-$  is reported in Figure 8. The higher amount of active chlorine confirms a better reactivity of chloride with the positively charged surface of  $\text{TiO}_2$  at 1.8 V.

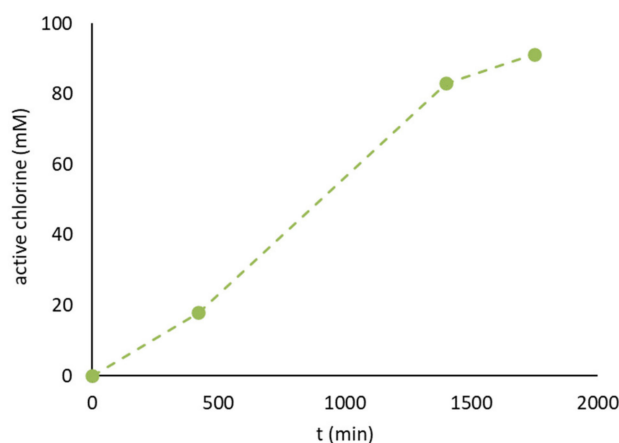


**Figure 8.** Trends with time of the concentration of active chlorine produced during a degradation run at 1.8 V with solution containing  $40 \text{ mg dm}^{-3}$  of DEP, 0.1 M  $\text{NaClO}_4$ , and 100 mM of  $\text{Cl}^-$ .

The formation of chlorine-based oxidants during photoelectrochemical treatment of water containing chloride has been studied by several authors: some of them found that the presence of  $\text{Cl}^-$  suppressed the degradation rate of organic pollutants, while others found opposed result [44].

The positive effect was generally observed when the active chlorine was able to give a bulk contribution to the reaction, i.e., in the cases where the organic pollutants can be oxidized also by active chlorine. For example, during photo-electrochemical discoloration of solutions containing Methylene Blue, low pH, and high concentration of  $\text{Cl}^-$  were beneficial [18]. Also, Zanoni et al. [17] found the highest TOC removal for solution containing Remazol Brilliant Orange 3R, working at pH 6.0, 1.0 M NaCl, when the photoelectrode was biased at +1 V (versus SCE).

In our case, the formation of active chlorine seems not sufficient to contribute to the overall reaction rate at such an extent to make up for the negative effect.

Some specific tests were performed to evaluate the effectiveness of the photo-electrogenerated active chlorine on the DEP degradation. To this aim, during photoelectrocatalytic degradation runs, the light was turned off and the application of bias potential was stopped. In

this condition, in the solution, 25  $\mu\text{M}$  of active chlorine accumulated, and residual 26  $\text{mg dm}^{-3}$  of DEP were present: the solution was monitored by following the concentration of the residual DEP with time. Negligible variation in the concentration of DEP was found after two hours indicating that the  $\text{HO}\bullet$  radicals may be considered as the main factor responsible for the degradation, while active chlorine seems to give a not significant contribution to the overall oxidation rate. Similar behavior was found during the electrochemical degradation of the dimethyl phthalate ester on a fluoride-doped  $\text{Ti}/\beta\text{-PbO}_2$  anode: the lower removal of the pollutant in the presence of chloride ions was explained considering the lower reactivity of dimethyl phthalate with chlorine radical species in respect to hydroxyl radicals. Also, the active chlorine can react with  $\text{HO}\bullet$  radicals thus reducing their availability for organic oxidation [46].

The low reactivity of active chlorine towards DEP obtained in our experimental conditions may indicate that the formation of harmful chlorinated intermediates is unlikely, even if the possible reaction of DEP intermediates with active chlorine during the runs cannot be excluded. Table 1 reports the ratio ( $\varphi$ ) between the removal percentages of TOC and DEP evaluated at the end of each run, which indicates the level of total mineralization as defined by the following equation [47]:

$$\varphi = \frac{\%[\text{TOC}]_{\text{removal}}}{\%[\text{DEP}]_{\text{removal}}} \quad (6)$$

**Table 1.** TOC removal and  $\varphi$  evaluated at the end of each run.

Applied Potential (V)	$[\text{Cl}^-]$ mM	TOC Removal	$\varphi$
0.2 V	0	31%	0.87
	1	28%	0.87
	100	26%	0.96
	500	11%	0.98
1.8 V	0	53%	0.96
	1	46%	0.99
	100	49%	1.00
	500	39%	1.00

At 1.8 V, a higher degree of mineralization was evaluated at the end of the runs, in which  $\varphi$  approached the unity. However, at 0.2 V, the high values of  $\varphi$  also indicate that the possible intermediates are almost completely removed.

#### 4. Conclusions

In this work, the photoelectrochemical degradation of diethyl phthalate has been studied at two levels of applied potentials and in the presence of different concentrations of chloride under simulated solar light conditions, using  $\text{TiO}_2$  nanotubular electrodes. The process is able to remove DEP following a pseudo-first order kinetics: values of  $k_{\text{app}}$  of  $1.25 \times 10^{-3} \text{ min}^{-1}$  and  $1.56 \times 10^{-4} \text{ min}^{-1}$  were obtained at applied potentials of 1.8 and 0.2 V, respectively. Higher current efficiency and slower kinetics of degradation were detected in the ohmic region of the polarization curve at 0.2 V. The presence of chloride ions in the solution affects the degradation rate to different extents depending of the applied potential: the higher the potential, the higher the negative effect of the increase of chloride concentration. The presence of 500 mM of  $\text{Cl}^-$  halves the  $k_{\text{app}}$  at 0.2 V, while at 1.8 V its value decreases to  $1.56 \times 10^{-4} \text{ min}^{-1}$ . This behavior can be connected to the blocking effect of adsorbed  $\text{Cl}^-$  and the competitive adsorption, with respect to water molecules, which reduces the formation of  $\text{HO}\bullet$  radicals: at 0.2 V, the adsorption of chloride predominates only at the highest concentration of chloride, while at 1.8 V, the positive surface charge due to the applied potential and the possible acidification of the anodic layer allow the adsorption also at low chloride concentrations.

**Author Contributions:** Conceptualization, A.V. and S.P.; methodology, M.M.; validation, L.M., A.V. and S.P.; formal analysis, L.M.; investigation, L.M.; writing—original draft preparation, A.V. and S.P.; writing—review and editing, S.P., L.M. and M.M. All authors have read and agreed to the published version of the manuscript.

**Funding:** This paper is part of the research project funded by P.O.R. SARDEGNA F.S.E. 2014–2020—Axis III Education and Training, Thematic Goal 10, Specific goal 10.5, Action partnership agreement 10.5.12—“Call for funding of research projects—Year 2017”.

**Data Availability Statement:** Data is contained within the article.

**Conflicts of Interest:** The authors declare no conflict of interest.

## References

1. Palmas, S.; Mais, L.; Mascia, M.; Vacca, A. Trend in using TiO<sub>2</sub> nanotubes as photoelectrodes in PEC processes for wastewater treatment. *Curr. Opin. Electrochem.* **2021**, *28*, 100699.
2. van de Krol, R. Principles of Photoelectrochemical Cells. In *Photoelectrochemical Hydrogen Production*; van de Krol, R., Grätzel, M., Eds.; Electronic Materials: Science & Technology; Springer: Boston, MA, USA, 2012; Volume 102, pp. 13–67.
3. Krivec, M.; Dillert, R.; Bahnemann, D.W.; Mehle, A.; Strancar, J.; Drazic, G. The nature of chlorine-inhibition of photocatalytic degradation of dichloroacetic acid in a TiO<sub>2</sub>-based microreactor. *Phys. Chem. Chem. Phys.* **2014**, *16*, 14867. [[CrossRef](#)] [[PubMed](#)]
4. Lin, L.; Jiang, W.; Chen, L.; Xu, P.; Wang, H. Treatment of produced water with photocatalysis: Recent advances, affecting factors and future research prospects. *Catalysts* **2020**, *10*, 924. [[CrossRef](#)]
5. Piscopo, A.; Robert, D.; Weber, J.V. Influence of pH and chloride anion on the photocatalytic degradation of organic compounds Part I. Effect on the benzamide and para-hydroxybenzoic acid in TiO<sub>2</sub> aqueous solution. *Appl. Catal. B Environ.* **2001**, *35*, 117–124. [[CrossRef](#)]
6. Selcuk, H.; Bekbolet, M. Photocatalytic and photoelectrocatalytic humic acid removal and selectivity of TiO<sub>2</sub> coated photoanode. *Chemosphere* **2008**, *73*, 854–858. [[CrossRef](#)]
7. Chong, M.N.; Jin, B.; Chow, C.W.K.; Saint, C. Recent developments in photocatalytic water treatment technology: A review. *Water Res.* **2010**, *44*, 2997–3027. [[CrossRef](#)]
8. Zhou, X.; Zheng, Y.; Zhou, J.; Zhou, S. Degradation kinetics of photoelectrocatalysis on landfill leachate using codoped TiO<sub>2</sub>/Ti photoelectrodes. *J. Nanomater.* **2015**, *2015*, 1–11. [[CrossRef](#)]
9. Konstantinou, I.K.; Albanis, T.A. TiO<sub>2</sub>-assisted photocatalytic degradation of azo dyes in aqueous solution: Kinetic and mechanistic investigations: A review. *Appl. Catal. B Environ.* **2004**, *49*, 1–14. [[CrossRef](#)]
10. Moser, J.; Gratzel, M. Photoelectrochemistry with colloidal semiconductors; laser studies of halide oxidation in colloidal dispersions of TiO<sub>2</sub> and  $\alpha$ -Fe<sub>2</sub>O<sub>3</sub>. *Helv. Chim. Acta* **1982**, *65*, 1436–1444. [[CrossRef](#)]
11. Ahmad, R.; Ahmad, Z.; Khan, A.U.; Mastoi, N.R.; Aslam, M.; Kim, J. Photocatalytic systems as an advanced environmental remediation: Recent developments, limitations and new avenues for applications. *J. Environ. Chem. Eng.* **2016**, *4*, 4143–4164. [[CrossRef](#)]
12. Sirtori, C.; Agüera, A.; Gernjak, W.; Malato, S. Effect of water-matrix composition on Trimethoprim solar photodegradation kinetics and pathways. *Water Res.* **2010**, *44*, 2735–2744. [[CrossRef](#)]
13. Brüninghoff, R.; van Duijne, A.K.; Braakhuis, L.; Saha, P.; Jeremiasse, A.W.; Mei, B.; Mul, G. Comparative Analysis of Photocatalytic and Electrochemical Degradation of 4-Ethylphenol in Saline Conditions. *Environ. Sci. Technol.* **2019**, *53*, 8725–8735. [[CrossRef](#)]
14. Peng, Y.P.; Yassitepe, E.; Yeh, Y.T.; Ruzybayev, I.; Shah, S.I.; Huang, C.P. Photoelectrochemical degradation of azo dye over pulsed laser deposited nitrogen-doped TiO<sub>2</sub> thin film. *Appl. Catal. B Environ.* **2012**, *125*, 465–472. [[CrossRef](#)]
15. Vacca, A.; Mais, L.; Mascia, M.; Usai, E.M.; Palmas, S. Design of experiment for the optimization of pesticide removal from wastewater by photo-electrochemical oxidation with TiO<sub>2</sub> nanotubes. *Catalysts* **2020**, *10*, 512. [[CrossRef](#)]
16. Pan, X.; Yang, M.Q.; Fu, X.; Zhang, N.; Xu, Y.J. Defective TiO<sub>2</sub> with oxygen vacancies: Synthesis, properties and photocatalytic applications. *Nanoscale* **2013**, *5*, 3601–3614. [[CrossRef](#)] [[PubMed](#)]
17. Zanoni, M.V.B.; Sene, J.J.; Anderson, M.A. Photoelectrocatalytic degradation of Remazol Brilliant Orange 3R on titanium dioxide thin-film electrode. *J. Photochem. Photobiol. A Chem.* **2003**, *157*, 55–63. [[CrossRef](#)]
18. Wu, X.; Huang, Z.; Liu, Y.; Fang, M. Investigation on the Photoelectrocatalytic Activity of Well-Aligned TiO<sub>2</sub> Nanotube Arrays. *Int. J. Photoenergy* **2012**, *2012*, 832516. [[CrossRef](#)]
19. An, T.; Zhang, W.; Xiao, X.; Sheng, G.; Fu, J.; Zhu, X. Photoelectrocatalytic degradation of quinoline with a novel three-dimensional electrode-packed bed photocatalytic reactor. *J. Photochem. Photobiol. A Chem.* **2004**, *161*, 233–242. [[CrossRef](#)]
20. Zhang, W.; An, T.; Cui, M.; Sheng, G.; Fu, J. Effects of anions on the photocatalytic and photoelectrocatalytic degradation of reactive dye in a packed-bed reactor. *J. Chem. Technol. Biotechnol.* **2005**, *80*, 223–229. [[CrossRef](#)]
21. Zanoni, M.V.B.; Sene, J.J.; Selcuk, H.; Anderson, M.A. Photoelectrocatalytic production of active chlorine on nanocrystalline titanium dioxide thin-film electrodes. *Environ. Sci. Technol.* **2004**, *38*, 3203–3208. [[CrossRef](#)]

22. Xu, B.; Gao, N.Y.; Sun, X.F.; Xia, S.J.; Rui, M.; Simonnot, M.O.; Causserand, C.; Zhao, J.F. Photochemical degradation of diethyl phthalate with UV/H<sub>2</sub>O<sub>2</sub>. *J. Hazard. Mater.* **2007**, *139*, 132–139. [[CrossRef](#)]
23. Chang, B.V.; Liao, C.S.; Yuan, S.Y. Anaerobic degradation of diethyl phthalate, di-n-butyl phthalate, and di-(2-ethylhexyl) phthalate from river sediment in Taiwan. *Chemosphere* **2005**, *58*, 1067–1601. [[CrossRef](#)]
24. Wang, H.; Sun, D.Z.; Bian, Z.Y. Degradation mechanism of diethyl phthalate with electrogenerated hydroxyl radical on a Pd/C gas-diffusion electrode. *J. Hazard. Mater.* **2010**, *180*, 710–715. [[CrossRef](#)] [[PubMed](#)]
25. Staples, C.A.; Peterson, D.R.; Parkerton, T.F.; Adams, W.J. The environmental fate of phthalate esters: A literature review. *Chemosphere* **1997**, *35*, 667–749. [[CrossRef](#)]
26. Staples, C.A.; Parkerton, T.F.; Peterson, D.R. A risk assessment of selected phthalate esters in North American and western European surface waters. *Chemosphere* **2000**, *40*, 885–891. [[CrossRef](#)]
27. Wang, R.; Ji, M.; Zhai, H.; Liub, Y. Occurrence of phthalate esters and microplastics in urban secondary effluents, receiving water bodies and reclaimed water. *Sci. Total Environ.* **2020**, *737*, 140219. [[CrossRef](#)]
28. Ma, F.; Shi, T.; Gao, J.; Chen, L.; Guo, W.; Guo, Y.; Wang, S. Comparison and understanding of the different simulated sunlight photocatalytic activity between the saturated and monovacant Keggin unit functionalized titania materials. *Colloids Surf. A Physicochem. Eng. Asp.* **2012**, *401*, 116–125. [[CrossRef](#)]
29. Cai, J.; Niu, B.; Zhao, H.; Zhao, G. Selective photoelectrocatalytic removal for group-targets of phthalic esters. *Environ. Sci. Technol.* **2021**, *55*, 2618–2627. [[CrossRef](#)]
30. Vacca, A.; Mais, L.; Mascia, M.; Usai, M.E.; Rodriguez, J.; Palmas, S. Mechanistic insights into 2,4-D photoelectrocatalytic removal from water with TiO<sub>2</sub> nanotubes under dark and solar light irradiation. *J. Hazard. Mater.* **2021**, *412*, 125202. [[CrossRef](#)] [[PubMed](#)]
31. Varghese, O.K.; Gong, D.W.; Paulose, M.; Grimes, C.A.; Dickey, E.C. Crystallization and high-temperature structural stability of titanium oxide nanotube arrays. *J. Mater. Res.* **2003**, *18*, 156–165. [[CrossRef](#)]
32. Allam, N.K.; El-Sayed, M.A. Photoelectrochemical water oxidation characteristics of Anodically Fabricated TiO<sub>2</sub> nanotube arrays: Structural and optical properties. *J. Phys. Chem. C* **2010**, *114*, 12024–12029. [[CrossRef](#)]
33. Palmas, S.; Da Pozzo, A.; Mascia, M.; Vacca, A.; Ardu, A.; Matarrese, R.; Nova, I. Effect of the preparation conditions on the performance of TiO<sub>2</sub> nanotube arrays obtained by electrochemical oxidation. *Int. J. Hydrogen Energy* **2011**, *36*, 8894–8901. [[CrossRef](#)]
34. Calza, P.; Pelizzetti, E. Photocatalytic transformation of organic compounds in the presence of inorganic ions. *Pure Appl. Chem.* **2001**, *73*, 1839–1848. [[CrossRef](#)]
35. Yang, S.; Chen, Y.; Lou, L.; Wu, X. involvement of chloride anion in photocatalytic process. *J. Environ. Sci.* **2005**, *17*, 761–765.
36. Burns, R.A.; Crittenden, J.C.; Hand, D.W.; Selzer, V.H.; Sutter, L.L.; Salman, S.R. Effect of inorganic ions in heterogeneous photocatalysis of TCE. *J. Environ. Eng.* **1999**, *125*, 77–85. [[CrossRef](#)]
37. Chen, H.Y.; Zahraa, O.; Bouchy, M. Inhibition of the adsorption and photocatalytic degradation of an organic contaminant in an aqueous suspension of TiO<sub>2</sub> by inorganic ions. *J. Photochem. Photobiol. A* **1997**, *108*, 37–44. [[CrossRef](#)]
38. Sunada, F.; Heller, A. Effects of water, salt water, and silicone overcoating of the TiO<sub>2</sub> photocatalyst on the rates and products of photocatalytic oxidation of liquid 3-octanol and 3-octanone. *Environ. Sci. Technol.* **1998**, *32*, 282–286. [[CrossRef](#)]
39. Abdullah, M.; Low, G.K.C.; Matthews, R.W. Effects of common inorganic anions on rates of photocatalytic oxidation of organic carbon over illuminated titanium dioxide. *J. Phys. Chem.* **1990**, *94*, 6820–6825. [[CrossRef](#)]
40. Azevedo, E.B.; de Aquino Neto, F.R.; Dezotti, M. TiO<sub>2</sub>-photocatalyzed degradation of phenol in saline media: Lumped kinetics, intermediates, and acute toxicity. *Appl. Catal. B* **2004**, *54*, 165–173. [[CrossRef](#)]
41. Adishkumar, S.; Kanmani, S.; Rajesh Banu, J. Solar photocatalytic treatment of phenolic wastewaters: Influence of chlorides, sulphates, aeration, liquid volume and solar light intensity. *Desalin. Water Treat.* **2014**, *52*, 7957–7963. [[CrossRef](#)]
42. Denisov, N.; Yoo, J.E.; Schmuki, P. Effect of different hole scavengers on the photoelectrochemical properties and photocatalytic hydrogen evolution performance of pristine and Pt-decorated TiO<sub>2</sub> nanotubes. *Electrochim. Acta* **2019**, *319*, 61–71. [[CrossRef](#)]
43. Peter, L.M.; Uppul Wijayantha, K.G.; Tahir, A.A. Kinetics of light-driven oxygen evolution at  $\alpha$ -Fe<sub>2</sub>O<sub>3</sub> electrodes. *Faraday Discuss.* **2012**, *155*, 309–322. [[CrossRef](#)]
44. Xiao, S.; Qu, J.; Liu, H.; Zhao, X.; Wan, D. Fabrication of TiO<sub>2</sub>/Ti nanotube electrode and the photoelectrochemical behaviors in NaCl solutions. *J. Solid State Electrochem.* **2009**, *13*, 1959–1964. [[CrossRef](#)]
45. Spadavecchia, F.; Ardizzone, S.; Cappelletti, G.; Falcicola, L.; Ceotto, M.; Lotti, D. Investigation and optimization of photocurrent transient measurements on nano-TiO<sub>2</sub>. *J. Appl. Electrochem.* **2013**, *43*, 217–225. [[CrossRef](#)]
46. Souza, F.L.; Aquino, J.M.; Irikura, K.; Miwa, D.W.; Rodrigo, M.A.; Motheo, A.J. Electrochemical degradation of the dimethyl phthalate ester on a fluoride-doped Ti/b-PbO<sub>2</sub> anode. *Chemosphere* **2014**, *109*, 187–194. [[CrossRef](#)] [[PubMed](#)]
47. Miwa, D.W.; Malpass, G.R.P.; Machado, S.A.S.; Motheo, A.J. Electrochemical degradation of carbaryl on oxide electrodes. *Water Res.* **2006**, *40*, 3281–3289. [[CrossRef](#)] [[PubMed](#)]